recovery energy environment economy
2011 CSPG CSEG CWLS Convention

Fracture Network of Synfolding in the Eastern Kohat Plateau, Northern Pakistan

Quaid Khan

NTC Building, 53,
G-5/2, Islamabad

Symmetric relations between synfolding fractures and fold geometry have been used to explain the formation of fracture in sedimentary rocks. Based on field observation - the spatial distribution of fracture system that has affected the Miocene Kamlial Formation of the Eastern Kohat syncline from foreland area of the Pakistani Himalaya. The syncline structure located in the East Kohat Potwar plateau.. .The dominant fracture trends are sub parallel and orthogonal to the fold hinge. The fracture system is dominated by near-orthogonal network of NE-SW and NW-SE striking fractures. The NE-SW fractures follow the axis of the syncline, whereas NW-SW fractures crosscut the fold axis. The scaling properties of these fracture system are analyzed from high quality, outcrop scale digital photographs of two locations, A and B. After digitization of fractures on commercially available drawing software, two dimension binary images were prepared for standard box-counting technique. The fracture sets are considered as a whole and not as an individual set of fractures. The results show that the spatial distribution of fractures and their growth follow power-law with fractal dimension (D) at location A (D = -1.153:10.057) and B (D = - 1.156:10.050), and have upper and lower fractal limit. The D values are effectively identical with minimum standard errors. The results conclusively suggest that there is a genetic link between the fractures from one location to another and that they developed synchronous with the folding event. The results have important implications on the geometry and growth propagation of the fracture development during folding, where the fracture sets are interpreted as tectonic in origin and are synchronous with the post-Miocene folding of the Kamlial Formation and are not pre- or post-folding fractures

INTRODUCTION

Eastern Kohat Geological fractures are discontinuous structures or discrete breaks within a rock mass that develop in response to stress. Fractures include faults, across which shear displacement occur; joints, which have an aperture but· show no significant shear displacement, and filled' structures, such as veins. They exist on a wide range of scales from microns to several hundreds of kilometers, and through out this scale range, fractures have a significant effect on crustal processes including fluid flow (e.g. hydrology and petroleum systems) and rock mechanics (e.g. slope stability) (see Barton & La Pointe, 1995; Turcotte, 1997). Conventional fracture analysis has typically been limited to the orientation distribution of fractures, for example, rose patterns, histograms and stereo plots. However, these techniques provide no significant information regarding their spatial distribution at different scales (see Gillespie et aI., 1993). In recent years, it has. been suggested that various techniques of fractals may usefully be applied to the study of spatial distribution of fractures, because similarities between small and large-scale fracture arrays have been found over many orders of magnitude (e.g. Bonnet, 2001). As defined by Gillespie et al., (1993), "a fractal

geometry is one which is scale independent or self-similar at all scales, such that any portion of the system is a scaled down version of the whole" or in other words "a fractal geometry represents the lack of any homogenization scale" (Bonnet et al., 2001). Several studies, using a variety of fractal techniques, have suggested that fracture patterns can be described by a unique fractal dimension, a parameter which is simply derived from the power-law exponent.

The purpose of this work is to test the power-law length scales of different sets of fractures that appear to be developed synchronous with the post-Miocene folding event of the Himalayan foreland. The study area is characterized by a map-scale synclinal structure, the Kushalgarh syncline (Fig. 1; Sayab & Jadoon, in review), where two major fracture sets affected the folded Miocene Kamlial Formation. Set 1 is oriented NE-SW, whereas set 2 is NW-SE. Standard box-counting technique is adopted (e.g. Gillespie et aI., 1993) for measuring the fractal dimension (D) of fractures. The results of the technique show that all the fractures have close genetic relationship and formed during folding (synfolding fractures) and follow power-law length scales, and have upper and lower fractal limits.

ATTRIBUTE OF SYNFOLDING FRACTURES

Location A

Detailed structural analyses of synfolding fractures developed in the Miocene Kamlial Formation in the Khushalgarh syncline are described in Sayab and Jadoon (in review).

Two key locations have been selected and briefly described in this paper (Fig. 2). The selection was made based on the quality of the outcrop exposure and exposed fractures. At location A (33°27.233 N;71°48.366 E) the strike of the bedding (SO) is ENE-WSW, moderately dipping towards NNW (Fig. 3b). Two major sets, have been observed. The dominant set (2), strike NE-SW (Fig. 3c). The frequency of fracture set 2 is high (0. *16f/meter)* with respect to the set 1. Most of the fractures of set '2 are planar or slightly undulating (terminology after Peacock et aI., 2000). In terms of fracture connectedness, their ends are free or some show one end connected. The least dominant set (1) is characterized by NW-SE striking fractures (Fig. 3c). They cross cut the bedding. The frequency of these fractures is low (0.04 *f/m)* as compared to set 2. They are slightly undulating or rarely undulating and connected with set 2 fractures, therefore" their ends are not free. Set 1 appears to be the latest as 'it cross cuts set 2 fractures. Outcrop observations suggest that the NE-SW fractures are mode I (tensile) fractures, whereas NW-SE fractures belong to mode II (shear) fractures.

Location B

Tectonic fractures were mapped and measured at a rectangle shaped outcrop face (33° 29.296 N; 71° 52.574 E)(Fig. 4a). The rectangle was ca. 390 cm long and 140 cm wide. Strike of the bedding (SO), which contains fractures, is NE-SW, moderately dipping towards NW. Altogether, 21 fractures were measured of different orientations and lengths. The dominant set is NW-SE followed by NE-SW, NS and W-E (Fig. 4b). The NW-SE trending fractures are moderately to steeply dipping either towards NE or SW, whereas NE-SW fractures are moderately to shallowly dipping towards SE (see also Sayab & Jadoon, this volume). N-S and E-W trending fractures moderately dipping towards the east and south, respectively. The fractures are slightly undulating and their ends are either ~connected or abut against the younger fractures. It is apparent from the outcrop that most of these fractures correspond to shear or mode II fractures.

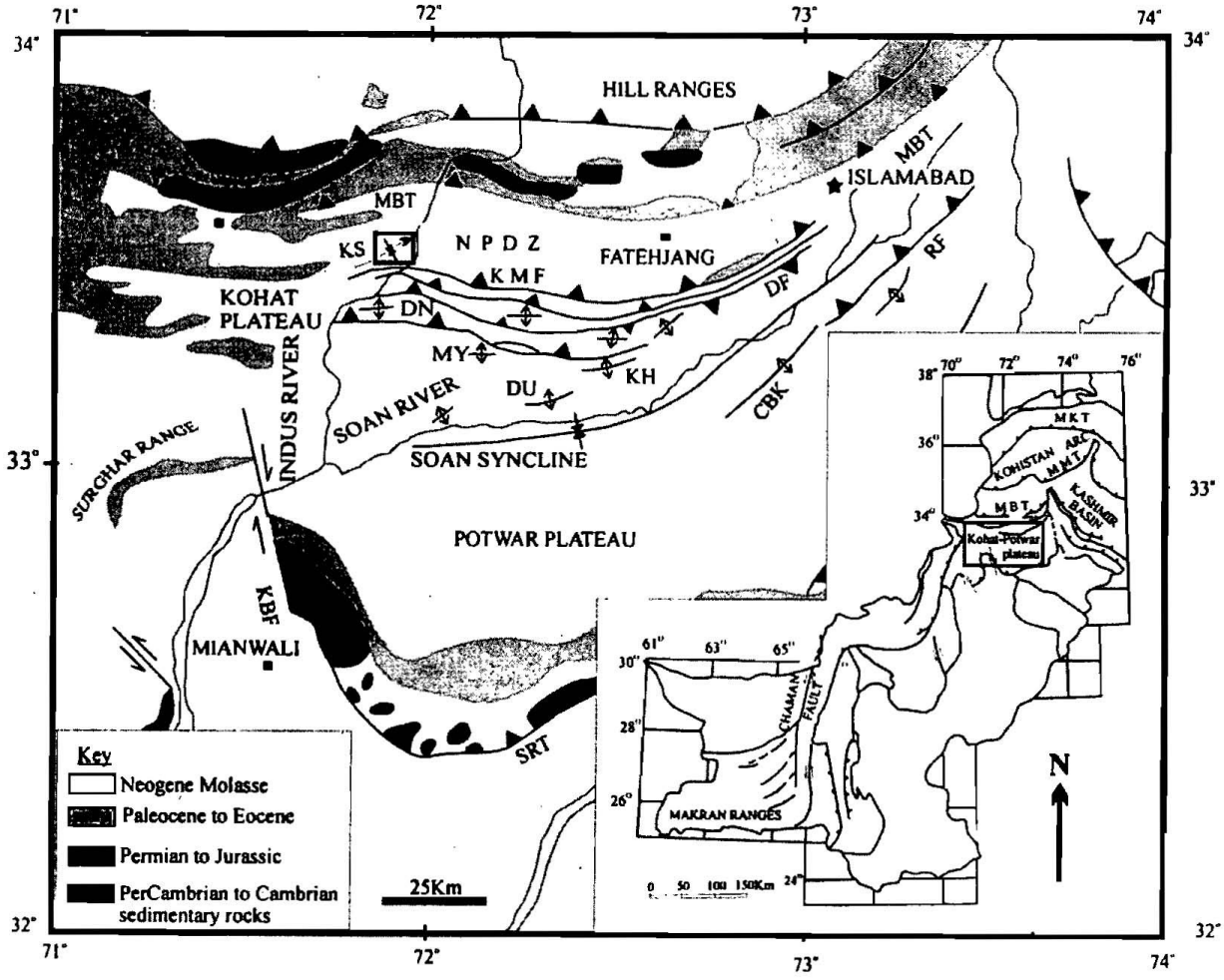

Fig. I. Generalized map of the Kohat, Potwar and Salt Range showing prominent tectonic features (after Jaswal et al., 1997). KS (Khushalgarh syncline (after Searle and Khan, not dated). CBK= Chak Beli Khan anticline, DF=Dhurnal Fault, DJ=Dil Jabba Fault, DN=Dakhni anticline, DU=Dhulian anticline, KBF=Kalabagh Fault, KH=Khaur . anticline, KMF= Kheri Murat· Fault, MBT = Main Boundary Thrust, MY = Meyal anticline, RF=Riwat Fault, SRT=Salt Range Thrust.

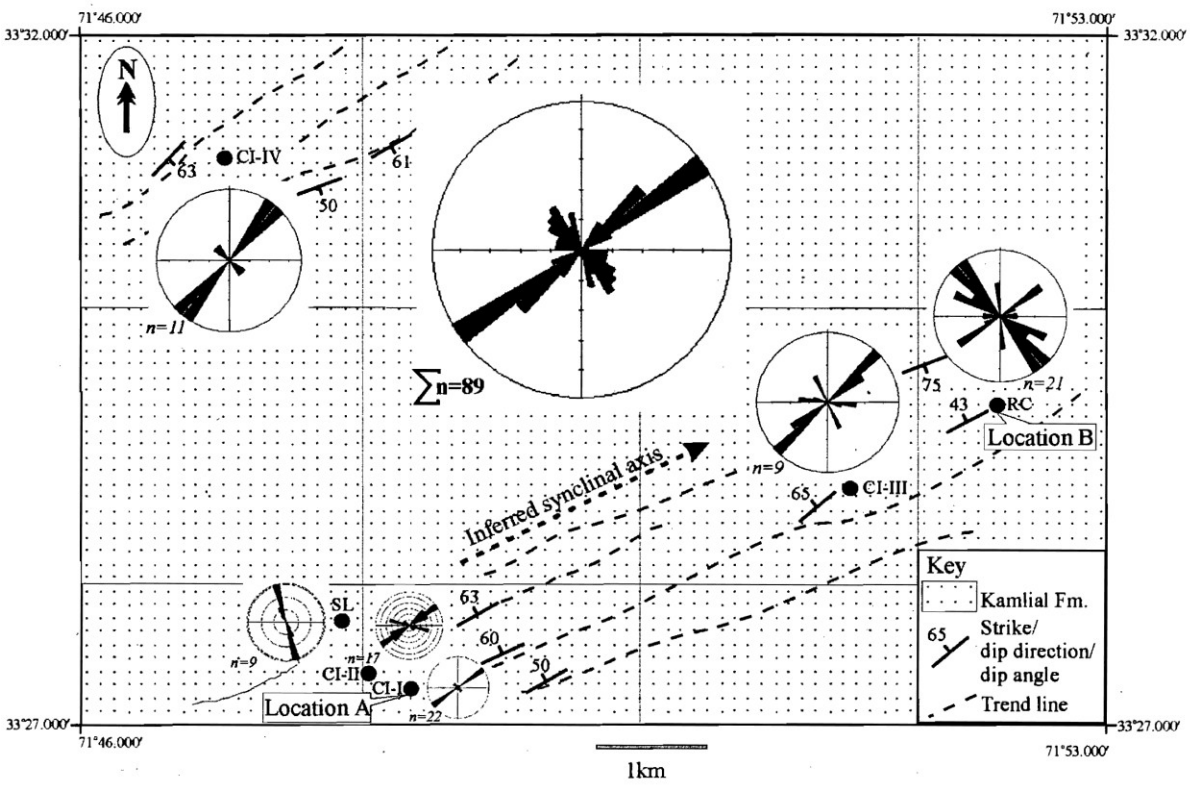

Fig. 2. Fracture pattern in the Kamlial Formation of the Eastern Kohat syncline (after Sayab & Jadoon, in review). Note, that the NESW fractures follow the axis of the fold, whereas NW-SE fractures cut fold axis at high angle. Inferred fold axis is after Searle & Khan (not dated). CI: circle inventory, SL: scan line, RC, rectangle.

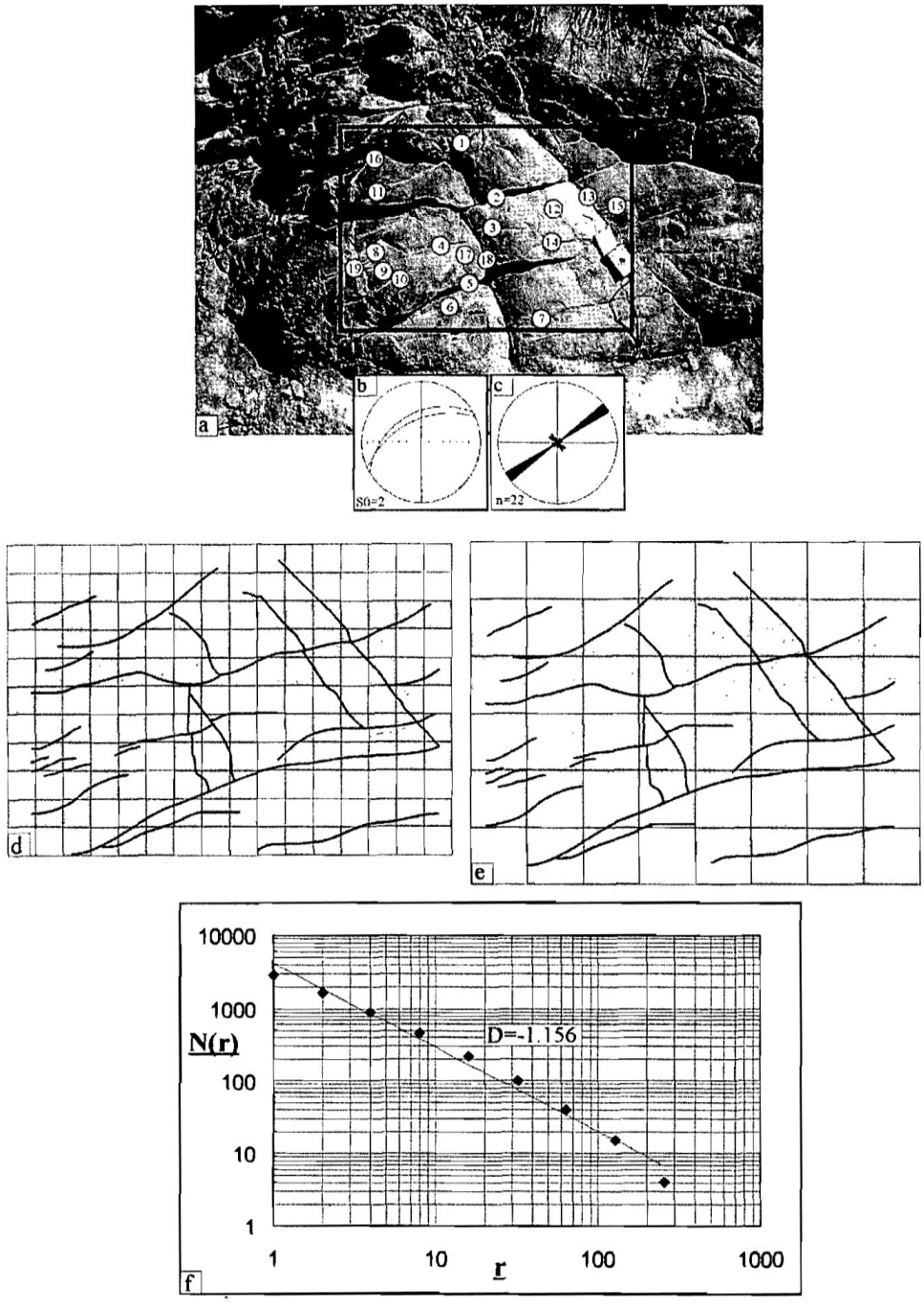

Fig. 3 (a) Fracture pattern from location A. Fractures are numbered for digitization. (b) Lower hemisphere equal area stereographic plot of *SO*. (c) Rose diagram showing fracture trends. (d and e) The box counting method for which the system is covered by a regular mesh of

size r. Two different mesh sizes are shown, where boxes inside which fractures are present are shaded. (t) Standard Box counting line for fracture patterns with D=-1.156.

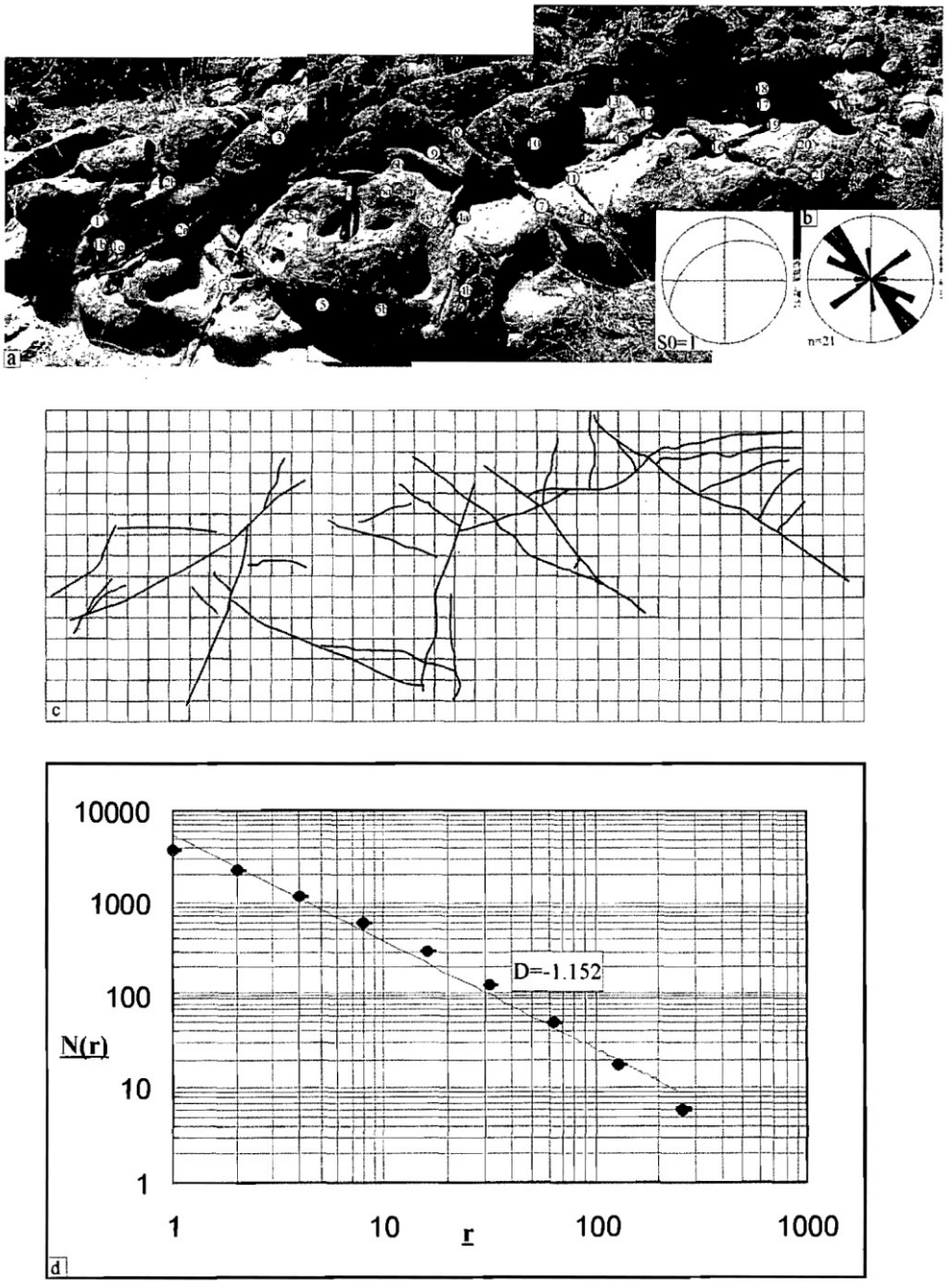

Fig. 4 (a) Fracture pattern from location B. Fractures are numbered for digitization. (b) Rose diagram showing fracture trends. (c) The box counting method for which the system is covered by a regular mesh of size r. Shaded boxes contain fractures. (I) Standard Box counting line for fracture patterns with D=-1.152.

METHOD

The mathematical theory of fractals is described by Mandelbrot (1982), and more information about fractals is given by Feder (1988) and Falconer (1990). In the case of fracture systems, Bonnet et al. (2001) defined two ways of measuring the fractals of the fracture patterns, (1) as a set of fractures, where each fracture (or fractures of distinct orientation) defines a separate object and (2) as a fractured domain, where the fracture pattern is considered as a whole. In this study, we have preferred and adopted the second case, as all the observed fractures in the Khushalgarh syncline appear to be synchronous with the folding (Sayab & Jadoon, in review).

The box-counting technique

In the box-counting method, the number of boxes of size *r, N(r),* required to cover the fractal object is counted (Fig. 3d,e) and should vary as:

$$N(r) \sim r^{-D}$$

Thus, by reporting *N(r)* versus *r* on a log-log plot, the fractal dimension *(D)* can be derived as the slope of the straight line. This method has been widely used to measure the fractal dimension of fractures networks (e.g., Mandelbrot, 1982; Hirata, 1989; Cello, 1997). The spatial distribution of fractures were analyzed using binary images of the 20 fracture photomosaics in the program ImageJ. The range of box size over which the data were linear was 2 to 256 units (Table 1). Regression between these two limits was used to derive the fractal dimensions with standard errors of regression.

Procedure

20 digitized fracture maps have been prepared from oriented field photographs. After digitization of fractures on commercially available drawing software, the fractures are overlaid with a grid of square boxes, where grids of different-size boxes are used (Fig. 3d,e & 4c) The number of boxes N of size r required to cover the fractures is then plotted on log-log graph as a function of r. The process was repeated for a range of values of r. The,N(r) versus r show a straight line is relationship on log-log plot.· From the slope of the line, applicable fractal dimension is obtained.

RESULTS

The results show that the fractal dimension of fractures at locations A (0 = -1.152) and B (D = -1.156) are effectively identical. Data points on a log-log plot are consistent within standard errors (Table I). The results conclusively suggest that there is a genetic link between the fractures that are developed during the folding event. It is further suggested that all the tectonic fracture sets are synchronous with the post-Miocene folding of the KamliaI Formation and are not pre- or post-folding and their spatial distribution follows power-law scales.

TABLE 1: LOG VALUES FOR NUMBER OF BOXES NR(Y) VERSUS BOX SIZE R (X)

X	Y
0	3.450249
0.30103	3.221153
0.60206	2.956649
0.90309	2.664642
1.20412	2.342423
1.50515	2
1.80618	1.60206
2.10721	1.176091
2.40824	0.60206

Location A, 0 = -1.156; standard error 0.057

X	Y
0	3.5669
0.60206	3.34811
0.90309	2.775246
1.20412	2.460898
1.50515	2.09691
1.80618	1.690196
2.10721	1.255273
2.40824	0.778151

Location A, 0 = -1.152; standard error 0.050

CONCLUSIONS

1 Following conclusions are drawn: 1) Box-counting analysis of fractures, exposed in the Eastern Kohat area, yield straight lines on log-log plots with similar fractal dimension number, hence implying that the fracture propagation during folding follows power law length scales.

2 The results suggest that the fractal dimension of fractures at two different locations is effectively identical and there is a genetic ·link between the fractures and are interpreted to be developed during the folding event and are not pre- or post-folding fractures.

Acknowledgements: Jadoon would like to acknowledge Dr Muhammad Sayab for useful discussions and guidance on fractals.

REFERENCES

Barton, c.c. & La Pointe P.R., 1995. Fractals in Petroleum geology and earth processes. Plenum Press, New York.

Bonnet, E., Bour, 0., Odling, N.E., Davy, P., Main, I. Cowie, P. & Berkowitz, B., 2001. Scaling of fracture systems in 8 geological media. Rew. Geophys., 39, 347-383.

Cello, G., 1997. Fractal analysis of a quaternary fault array in the central

Apennines, Italy. J. Struct. Geol., 19, 945-953.

Falconer, K., 1990. Fractal geometry: mathematical foundations and applications. John Wiley, New York. Feder, J., 1988. Fractals. Plenum, New York.

Gillespie, P.A., Howard, C.B., Walsh, 1.1. & Watterson, J., 1993. Measurement and characterization of spatial distributions of fractures. Tectonophys., 226, 113-141.

Hirata, T. '. 1989. Fractal dimension of fault system in Japan: fractal structure in rock fractures in rock fracture geometry at various scales. Pure Appl. Geophys., 131,157-169.

Jaswal, T.M., Lillie, R.J. & Lawrence, R.D., 1997. Structure and evolution of the Northern Potwar Deformed Zone, Pakistan. Am. Assoc. Petrol. Geol. Bull., 81, 308-382.

Mandelbrot, B.B., 1982. The fractal geometry of nature. Freeman, New York.

Peacock, D.C.P., Knipe, R.J. & Sanderson, 0.1.,2000. Glossary of normal faults. J. Struct. Geol., 22, 291-305.

Sayab, M. & Jadoon, Q.K., (this volume). Kinematics of tectonic fracture development during regional folding in sandstones of the Kamlial Formation, NWFP, northern Pakistan. Geol. Bull. Univ. Peshawar.

Searle, M.P. & Khan, M.A., (1995). Geological map of North Pakistan. Turcotte, D.L., 1997. Fractals and chaos in geology and geophysics. Cambridge University Press, Australia.